

Supporting Information

A Highly Permeable Fluorinated Polymer Nanocomposite for Plasmonic Hydrogen Sensing

I. Östergren,¹⁺ A. M. Pourrahimi,¹⁺ I. Darmadi,²⁺ R. R. da Silva,¹ A. Stolaś,¹ S. Lerch,¹ B. Berke,² M. Guizar-Sicairos,³ M. Liebi,² G. Foli,⁴ V. Palermo,^{4,5} M. Minelli,⁶ K. Moth-Poulsen,^{1*} C. Langhammer,^{2*} C. Müller^{1*}

¹Department of Chemistry and Chemical Engineering, Chalmers University of Technology, 412 96 Göteborg, Sweden

²Department of Physics, Chalmers University of Technology, 412 96 Göteborg, Sweden

³Paul Scherrer Institut, PSI-Villigen, Switzerland

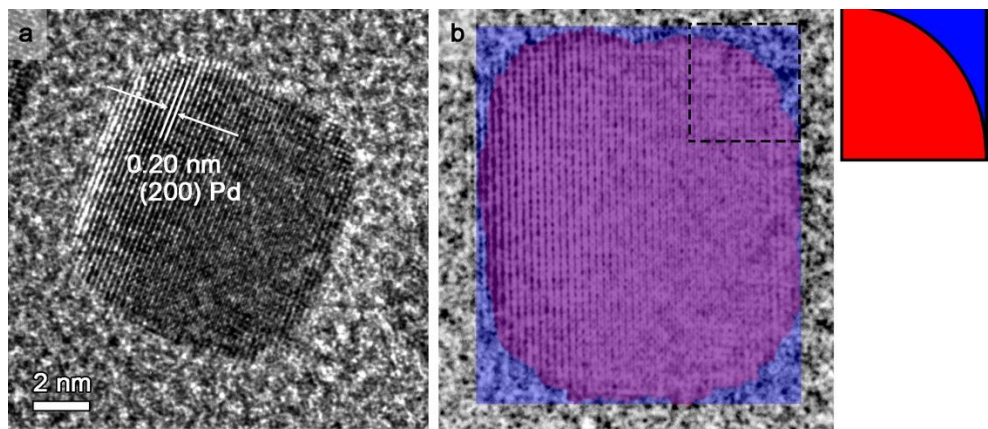
⁴ Institute of Organic Synthesis and Photoreactivity, National Research Council, 40129, Bologna, Italy

⁵ Department of Industrial and Materials Science, Chalmers University of Technology, 412 96 Göteborg, Sweden

⁶Department of Civil, Chemical, Environmental and Materials Engineering, Alma Mater Studiorum - University of Bologna, 40131 Bologna, Italy

⁺equal contribution

*Correspondence to: moth-poulsen@chalmers.se, christian.muller@chalmers.se, clangham@chalmers.se



Blue Area = Expected area coverage for 100% sharp nanocube
Red Area = Area covered by truncated nanocube
$$\% \text{ Truncation} = \frac{\text{Blue Area} - \text{Red Area}}{\text{Blue Area}} \times 100$$

Figure S1. a) High-resolution TEM image of a single Pd nanocube, and b) calculation of edge-truncation degree of a single nanocube. The nanocubes showed ~15% of edge-truncation.

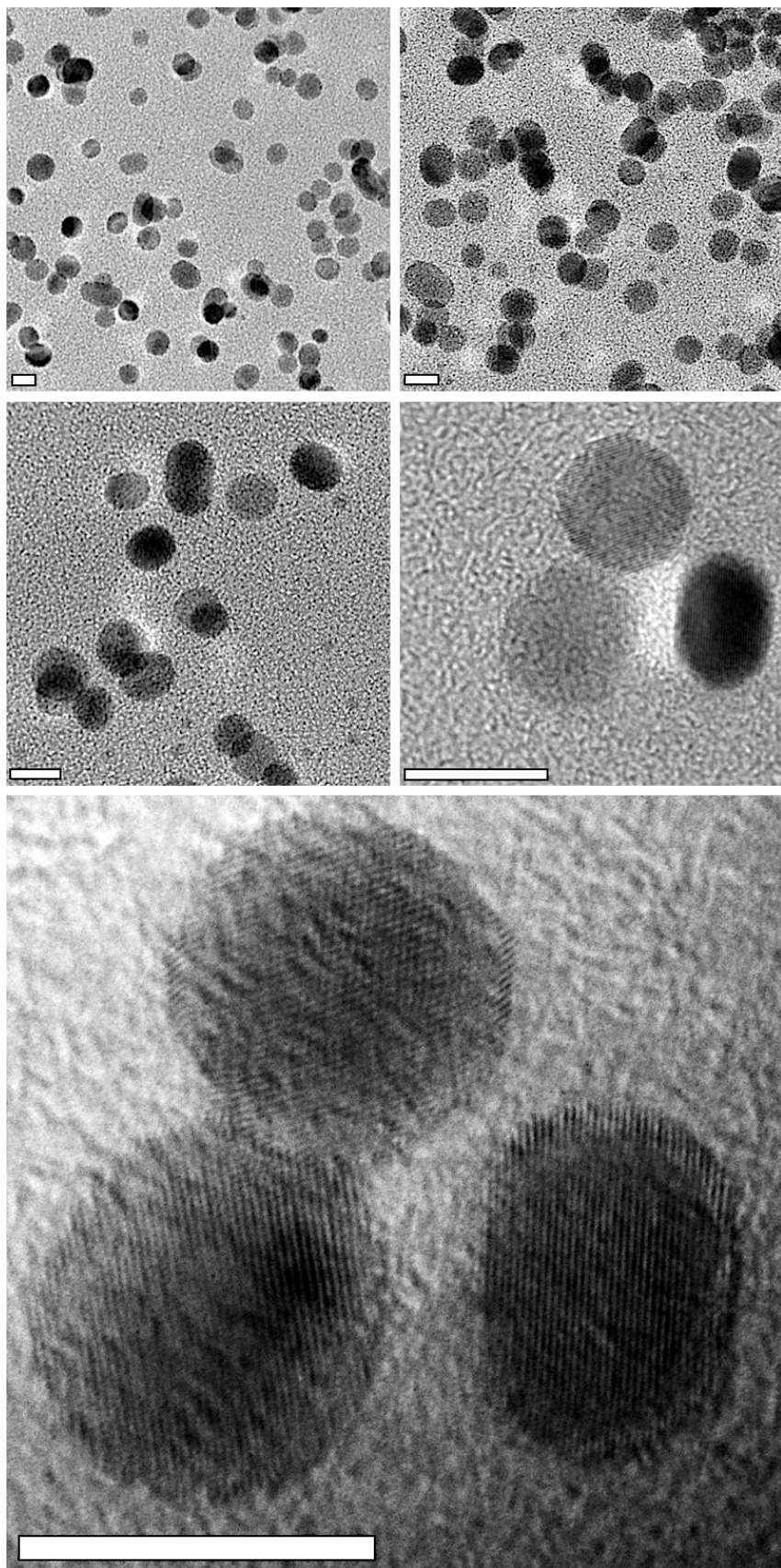


Figure S2. TEM images (different magnifications) taken from dispersed Pd nanoparticles in Teflon AF. Scale bars are 10 nm. Pd content $\sim 8 \times 10^{-3}$ vol. %.

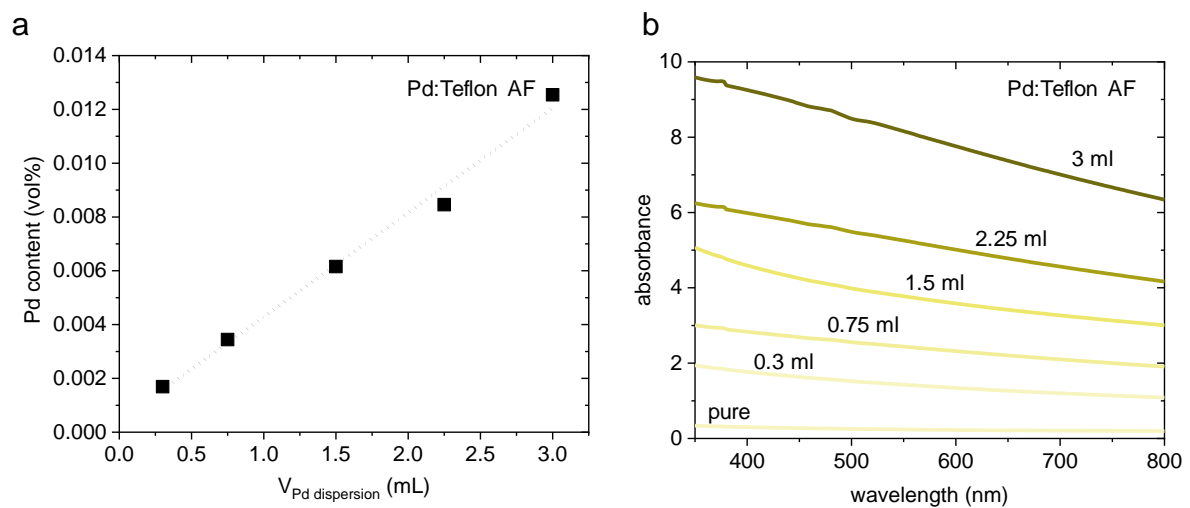


Figure S3. a) The Pd nanocube concentration in Pd:Teflon AF nanocomposites versus added volume of Pd nanocube suspension (isopropanol medium) after flow synthesis and medium exchange; b) UV-vis absorbance spectra of 100 μm thick Pd:Teflon AF nanocomposite plates with different added volume of Pd nanocube suspension (isopropanol medium).

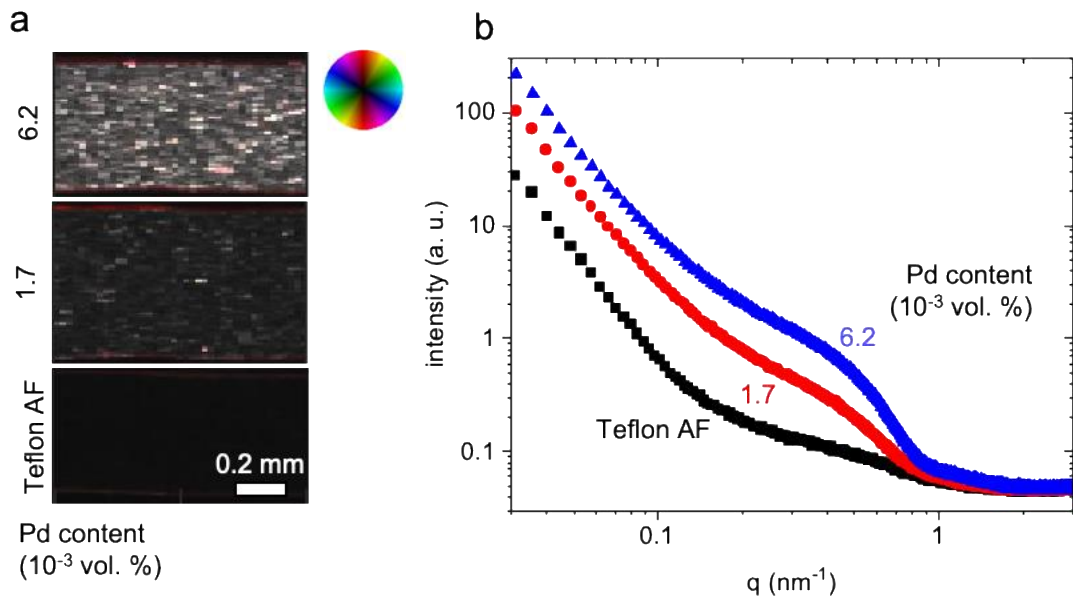


Figure S4. Small-angle X-ray scattering (SAXS) of Pd:Teflon AF nanocomposites. a) combined scanning-SAXS images of melt-pressed (combine the preferred orientation angle, the degree of orientation and the average scattering intensity in a hue-saturation-value representation according to the color wheel analyzed in a q -range of 0.2 to 0.69 nm^{-1}) and b) SAXS scattering curves of Pd:Teflon AF nanocomposites (raw data, i.e. before subtraction). Blue triangles correspond to a 6.2×10^{-3} vol % Pd particles and red circles to 1.7×10^{-3} vol % Pd particles.

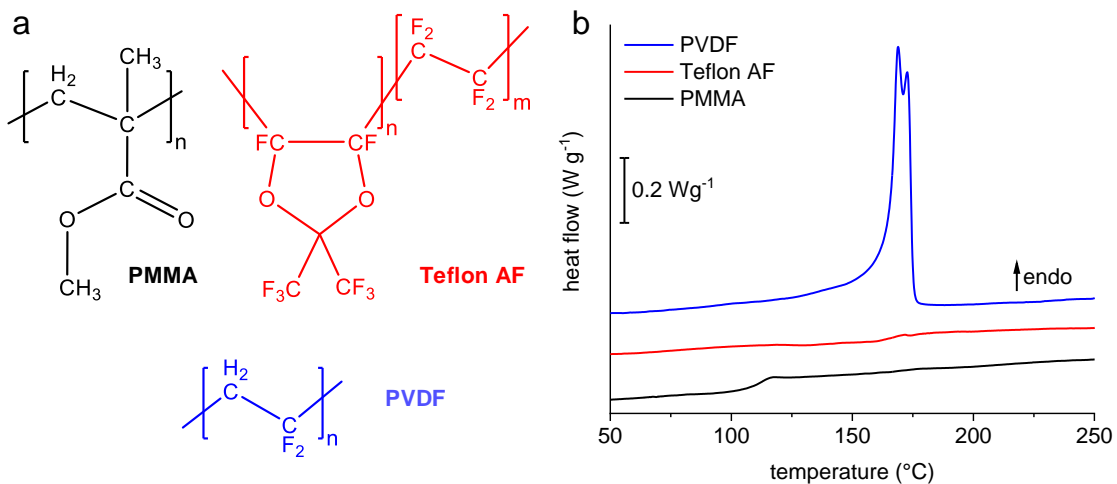


Figure S5. a) Chemical structure and b) heating DSC thermograms of PMMA, Teflon AF and PVDF.

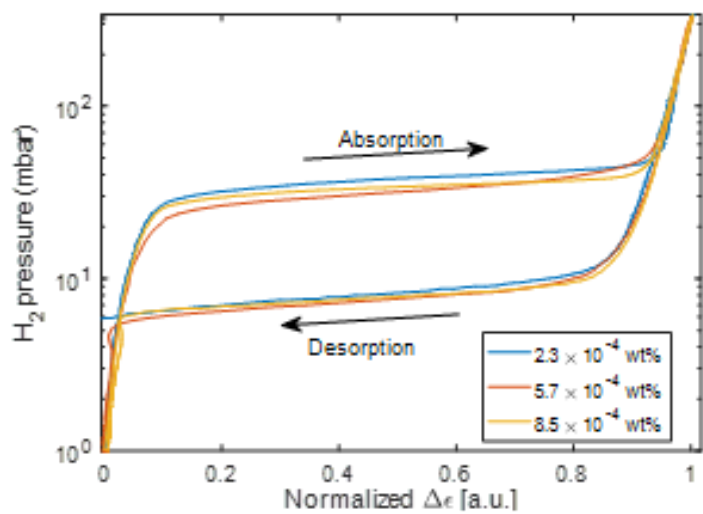


Figure S6. The pressure-composition isotherms of different Pd concentration in Teflon AF.

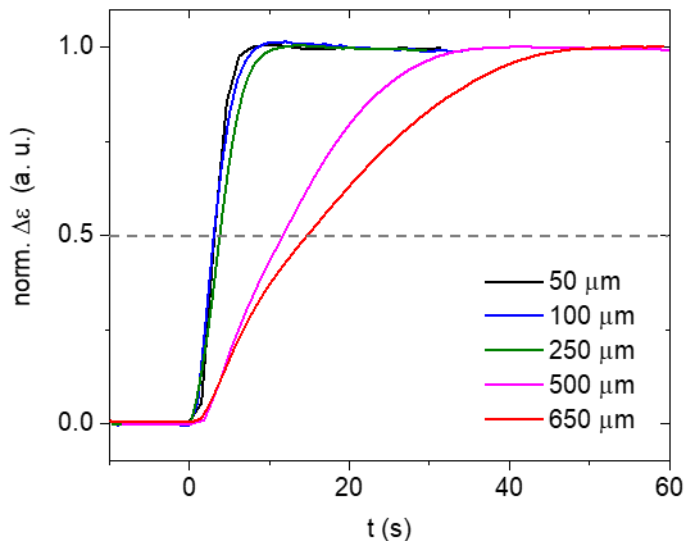


Figure S7. Normalized $\Delta\epsilon$ of melt-pressed Pd:Teflon AF (3.4×10^{-3} vol. % Pd) plates upon a sudden increase in H_2 pressure from 0 to 100 mbar H_2 (the H_2 valve opens at $t = 0$).

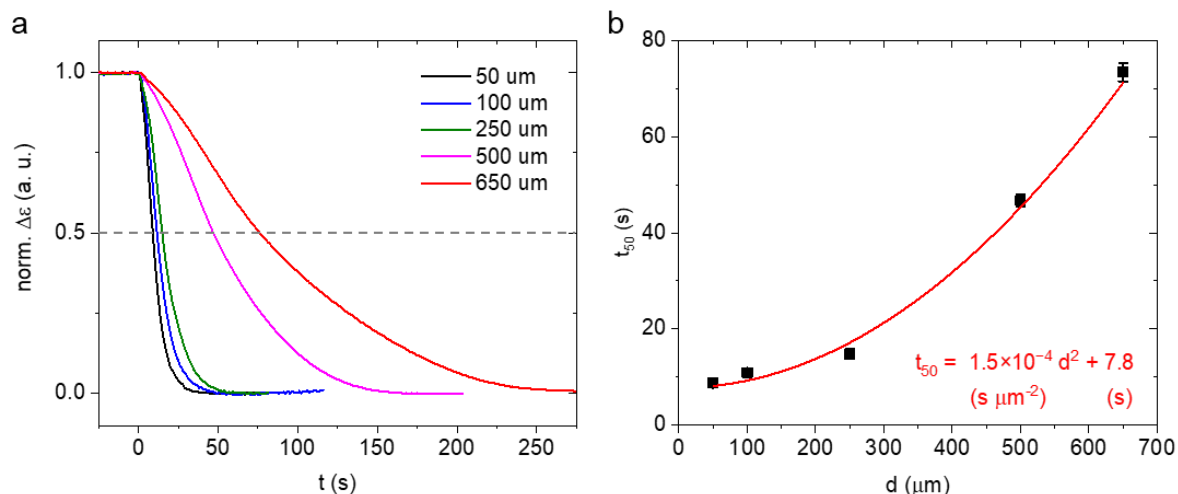


Figure S8. a) Normalized $\Delta\epsilon$ of melt-pressed Pd:Teflon AF (3.4×10^{-3} vol. % Pd) plates during desorption; b) Corresponding sensor response time (H_2 desorption time) t_{50} .

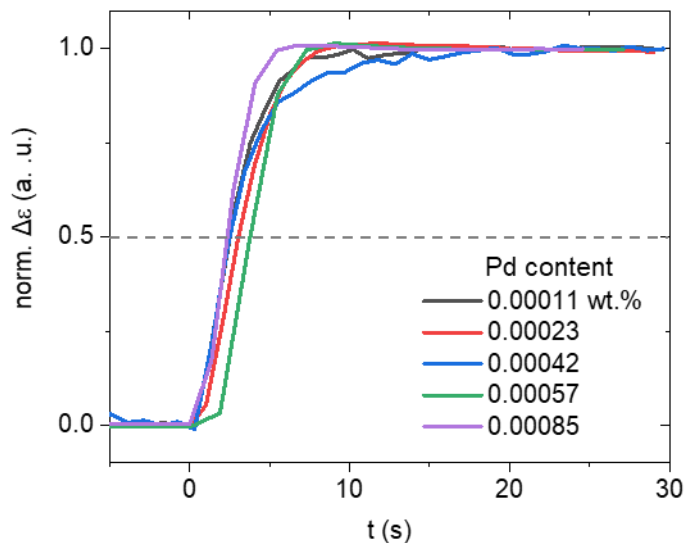


Figure S9. Normalized $\Delta\epsilon$ of 100 μm thick melt-pressed Pd:Teflon AF plates with different Pd content.

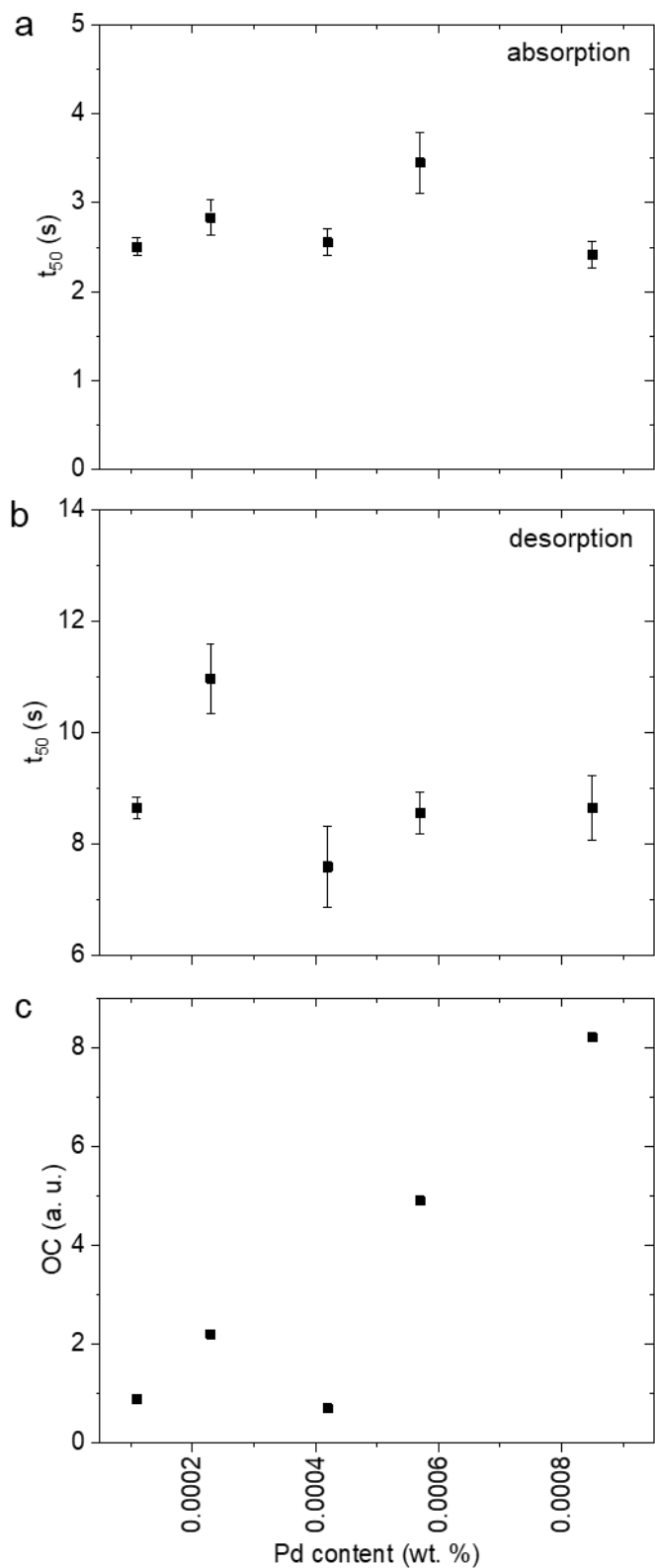


Figure S10. a) and b) H_2 absorption and desorption time (t_{50}), respectively and c) optical contrast of 100 μm thick melt-pressed Pd:Teflon AF plates with different Pd content.

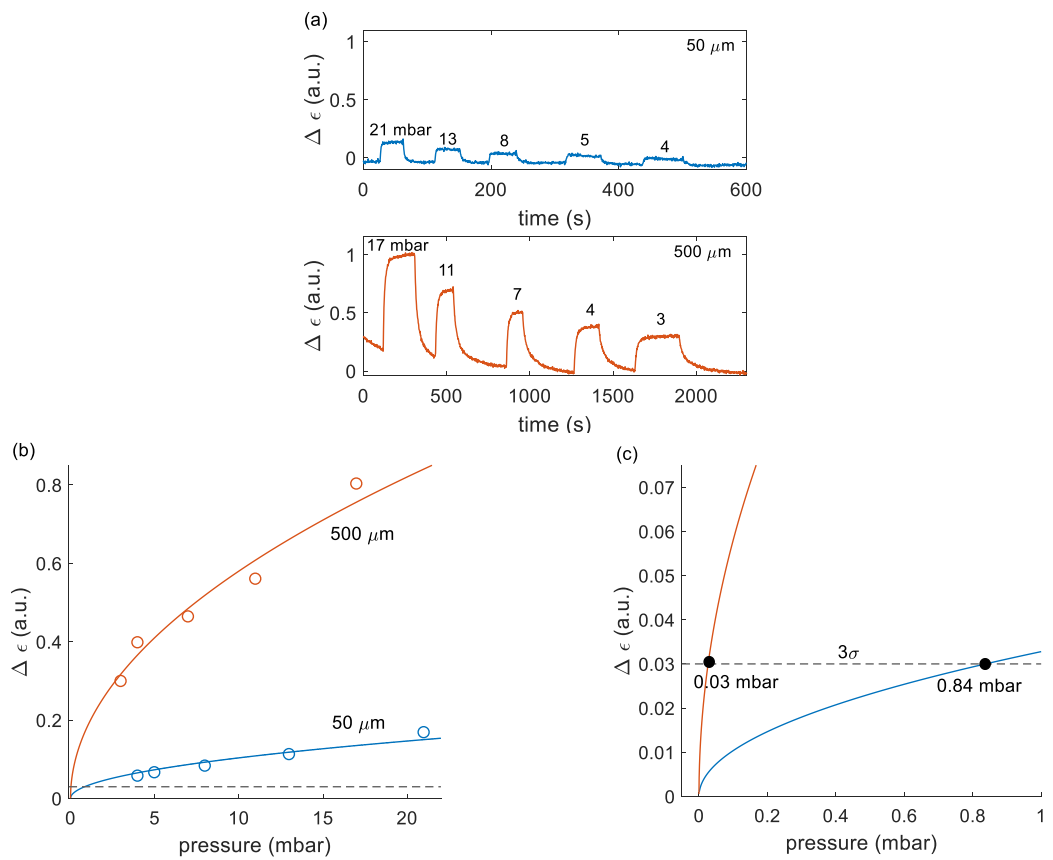


Figure S11. a) Sensor response of 50 and 500 μm thick sensor at low hydrogen pressures, b) the optical responses ($\Delta \epsilon$) vs hydrogen pressure and c) a magnification of b) at very low pressure.

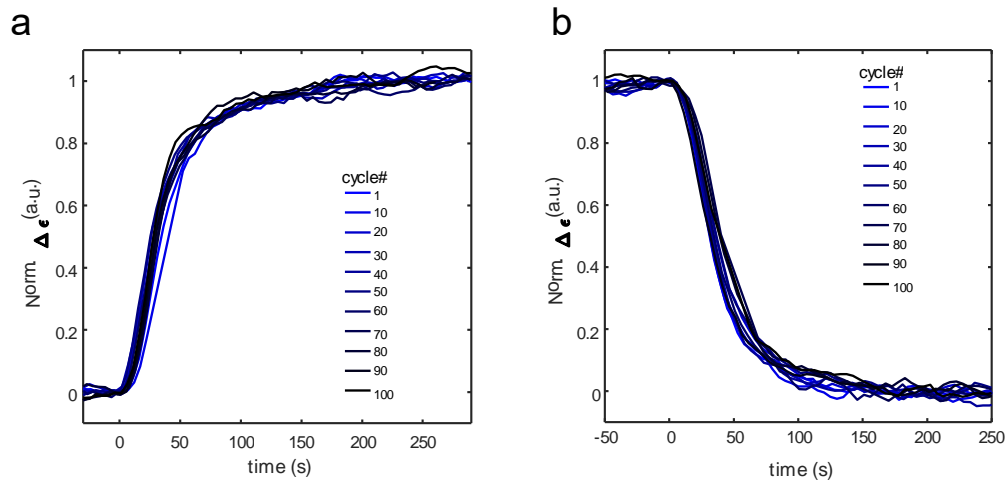


Figure S12. Normalized $\Delta\epsilon$ of optical fiber cap Pd:Teflon AF (3.4×10^{-3} vol. % Pd) a) absorption and b) desorption during cyclic exposure to 4 vol% hydrogen in synthetic air.